PCCP

pH and Ca^{2+} dependent interaction of Annexin V with phospholipid membranes: a combined study using fluorescence techniques, microelectrophoresis and infrared spectroscopy

H. Binder,* G. Köhler, K. Arnold and O. Zschörnig

University of Leipzig, Department of Medicine, Institute of Medical Physics and Biophysics, Liebigstr. 27, D-04103 Leipzig, Germany. E-mail: binder@rz.uni-leipzig.de

Received 14th April 2000, Accepted 21st August 2000
First published as an Advance Article on the web 27th September 2000

Annexins comprise a family of proteins that is possibly relevant to *in vivo* functions such as the formation of Ca^{2+} channels. The current work was undertaken to study the effect of annexin V (AxV) on vesicle fusion and/or destabilization, and on the phase behavior of the lipid in neutral and acidic conditions. Several techniques capable of providing information from lipid bilayer and multilayer systems were utilized to study the interaction of AxV with phosphatidylserine (PS) membranes as a function of Ca^{2+} concentration and pH. Microelectrophoresis indicates nearly complete binding of AxV to PS vesicles in the presence of Ca^{2+}. Quenching of tryptophan fluorescence of AxV by doxyl radicals attached at different positions of the lipid chains indicates partial penetration of AxV near the glycerol region of the lipid. Dansyl fluorescence shows that the apparent relative permittivity in the headgroup region of the lipid decreases upon Ca^{2+} and pH-mediated binding of AxV. The additives AxV and Ca^{2+} cause the destruction of vesicles in the first place and their fusion only to a weaker degree at neutral pH. Phase behavior and details of headgroup structure were studied by IR spectroscopy. In neutral conditions ternary complex formation between the anionic binding sites of AxV, negatively charged PS headgroups and calcium ions stabilizes the gel state of the lipid. The effect of the divalent cations on the membranes is amplified in the presence of the macromolecules. At pH 5 AxV shifts the phase transition temperature of PS downwards. AxV destroys the integrity of PS vesicles in acidic conditions, even in the absence of Ca^{2+}. These effects can be explained by an increased hydrophobicity of the protein at low pH. Binding of AxV to lipids becomes progressively driven by the hydrophobic effect with decreasing pH whereas the role of Ca^{2+}-mediated interactions decreases. We suggest that a peripheral calcium mediated insertion mode of AxV at neutral pH shifts towards a more integral one at acidic pH.

1. Introduction

Annexin V (AxV) is a member of a structurally homologous group of proteins that bind to phospholipid membranes in a calcium-dependent manner. Different biological functions such as an involvement in exocytosis, membrane trafficking, coagulation or Ca^{2+}-channel activity have been discussed (for a review see ref. 1). The crystal structures of annexins revealed a core tetrad of domains each containing a four-helix bundle with a fifth "capping" helix connected by short coil segments.[2] These interhelical loops represent binding sites for calcium. The protein surface which coordinates calcium ions is the feature which binds to phospholipid membranes *via* Ca^{2+} bridges.[3,4]

At neutral pH calcium ions are required to induce significant binding of AxV to negatively charged membranes.[5] The affinity of AxV for membranes is negligible in the absence of Ca^{2+} but strongly increases in acidic conditions because of the hydrophobization of the protein surface. For the matrix vesicle annexin (Anchorin CII), which shares close homology with AxV, a partitioning into lipophilic milieu under acidic conditions has been reported.[6] These findings suggest that AxV can induce structural changes of the hydrophobic core of lipid membranes. This property is thought to allow specific members of the annexin family to transverse the membrane in order to form Ca^{2+} channels, to assume proteolipid-like properties, or to become externalized.

The current work reports a joint study which was undertaken to address three major issues: (i) the consequences of AxV binding to lipid membranes in neutral and acidic conditions on a molecular level; (ii) the consequences of AxV binding at neutral and acidic conditions with respect to vesicle fusion and/or destabilization; and (iii) the effect of AxV binding in neutral and acidic conditions on the phase behavior of the lipid.

Several techniques capable of providing information from lipid bilayer and multilayer systems were utilized to study the interaction of AxV with phosphatidylserine membranes as a function of Ca^{2+} and pH. Electrophoretic mobility of lipid vesicles was measured to estimate AxV binding and its consequence for surface electrostatics. Fluorescence techniques are expected to yield information about the degree of incorporation of AxV into the membrane core and about the degree of hydrophobization of the polar region of the bilayer after AxV binding. Fluorescence leakage and content mixing assays provide information about bilayer stability and about aggregation and fusion of vesicles. IR spectroscopy permits one to detect phase transitions and additive-induced perturbations at particular lipid sites to be directly detected without use of probe molecules.

2. Materials and methods

Materials and preparation of lipid vesicles

Sodium salts of bovine brain phosphatidylserine (BBPS) and of dimyristoyl phosphatidylserine (DMPS) were purchased from Avanti Polar Lipids (Alabaster, Ala, USA) and used for fluorescence, electrophoresis (BBPS) and IR (DMPS) measurements. Recombinant human Annexin V, purified from *Escherichia coli*, was obtained from Serva (Heidelberg, Germany). Dansylphosphatidylethanolamine (DPE) was from Sigma (Deisenhofen, Germany) and 1-palmitoyl-2-(*n*-doxylstearoyl)-sn-glycero-3-phosphatidylcholine with $n = 5$, 12, 16 from Avanti Polar Lipids. The water soluble fluorescent probe 8-aminonaphthalene-1,3,6-trisulfonic acid (ANTS) and the quencher *p*-xylene-bis-pyridinium bromide (DPX) for leakage and contents mixing experiments were purchased from Molecular Probes (Eugene, USA).

For preparation of large unilamellar vesicles (LUV) the lipid in a chloroform–methanol stock solution (1 : 3 v/v), was dried and re-suspended by vortexing in buffer solution followed by five freeze–thawing cycles and by extrusion (Lipex extruder, Biomembranes, Vancouver, Canada) of the suspension through a polycarbonate Nucleopore membrane (100 nm pore-size, Millipore).[5] For mixing and leakage experiments the vesicles were eluted through Sephadex G50 gel chromatogaphy columns (Pharmacia, Sweden). Different buffer solutions containing 100 mM NaCl were used for sample preparation: 10 mM citrate (pH 3.5–5), MES (5–6) and HEPES (7.0–7.4).

For IR measurements, small unilamellar vesicles (SUV) of DMPS were prepared by sonication of the lipid suspension in buffer. Protein and/or $CaCl_2$ solutions in the same buffer medium were added after sonication. The final concentrations of the SUV samples were ~5 mM DMPS, ~2 μM AxV and 1 mM Ca^{2+}.

Microelectrophoresis and surface charge density

The electrophoretic mobility of BBPS LUV was measured using a Malvern Zetasizer 4 device. The modulation frequency was 250 Hz and the electrode current 7.5 mA. The ζ potential, is directly related to the electrophoretic mobility $b = v/E$ (v is the velocity of the particle and E the electric field strength) according to the Helmholtz–Smoluchowski equation, $\zeta = b\eta/(\varepsilon_0\varepsilon_r)$ (η is the viscosity, ε_0 the absolute and ε_r the relative permittivity of the medium). The surface potential of the vesicles was estimated by means of $\Psi_0 = (2RT/F)\ln\{(1 + q\exp(r/l_D))/(1 - q\exp(r/l_D))\}$ with $r \approx 0.2$ nm and $q = (\exp(F\zeta/2RT) - 1)/(\exp(F\zeta/2RT) + 1)$. R, F and T denote the gas constant, the Faraday constant and the temperature, respectively. The Debye length and the ionic strength are given by $l_D = (\varepsilon_0\varepsilon_r RT/2IF^2)^{0.5}$ and $I = 0.5\Sigma z_i^2 c_i$ (summation runs over the charge, z_i, and the concentration, c_i, of all ions present in the solution), respectively. Finally, the apparent surface charge density is given by

$$\sigma_{ap} = (2\varepsilon_0\,\varepsilon_r RT\Sigma c_i(\exp(-z_i F\Psi_0/RT) - 1))^{0.5}. \quad (1)$$

In a first-order approximation the apparent charge density can be written as the sum of the contribution of the PS moieties, the bound Ca^{2+} ions and the bound AxV molecules:

$$\sigma_{ap} = \sigma_{PS} + \sigma_{ax} + \sigma_{Ca}. \quad (2)$$

σ_{PS} was determined from the ζ potential of PS LUV in the absence of Ca^{2+} ions. Consequently, the increment of surface charge density after addition of Ca^{2+} is $\sigma_{Ca} = \sigma_{ap} - \sigma_{PS} = 2e[Ca^{2+}]_{bound}/(0.5[PS]A_L)$. After rearrangement one obtains an estimate of the amount of calcium cations which bind to the outer surface of the vesicles, $[Ca^{2+}]_{bound}$. The area per lipid in the membrane plane was set to $A_L = 0.7$ nm^2. The increment of surface charge due to the protein is related to the protein concentration by $\sigma_{ax} \approx ez_{ax}[AxV]/(0.5[PS]A_L)$ where z_{ax} denotes its effective charge.

The analysis in terms of the Helmholtz–Smoluchowski equation predicts that the electrophoretic mobility of a particle should be independent of its size and shape for all charge densities. This is approximately the case for phospholipid vesicles in decimal molar salt solutions.[7] Consequently, our analysis is expected to be independent of aggregation and fusion of vesicles.

Fluorescence measurements: Quenching, surface relative permittivity, leakage and contents-mixing

Trp-187-fluorescence of AxV was quenched by doxyl spin-probes at the position 5, 12 and 16 of the C18 chains of a C18–C16 di-acyl lipid with phosphocholine (PC) headgroup. The composition of BBPS : doxyl-PC vesicles was 1 : 1 mol/mol (100 μM total lipid concentration). Tryptophan fluorescence was excited at 280 nm and detected at 330 nm. In addition, the water soluble quencher acrylamide was used to study the accessibility of Trp-187 for the water phase.

Stock solutions of DPE and of BBPS were mixed to yield a molar ratio BBPS/DPE of 200–300 for the measurement of surface relative permittivity. The fluorescence spectra of DPE in aqueous LUV suspensions were measured with excitation at 340 nm. The wavelength at maximum fluorescence intensity is related to the apparent relative permittivity of the probe environment which was normalized by use of a set of organic solvents.[8] Typically, a blue shift of the emission maximum indicates a decrease in the surface relative permittivity.

Contents-mixing and leakage assays are based on the quenching of the water-soluble fluorophore ANTS by DPX.[9] For the first method two populations of LUV containing either the quencher (90 mM) or the fluorophore (25 mM) were mixed (1 : 1). The total fluorescence intensity of ANTS (excitation at 360 nm and emission >530 nm) was measured as a function of time. Upon contents mixing the fluorescence intensity decreases because the quencher content mixes with the fluorophore content. The degree of contents-mixing is given by

$$D = 100(I_\infty - I_0)/(I_R - I_0) \quad (3)$$

where I_0 and I_∞ denote the fluorescence intensity immediately before the mixing of the vesicles and after equilibration of the mixed system, respectively. The reference intensity, I_R, was obtained from vesicles which contain a mixture of ANTS and DPX in the respective concentrations.

For leakage experiments the LUV were filled with a solution of 12.5 mM ANTS and 20 mM DPX which guarantees strong quenching of fluorescence. Leakage induces dilution of the quencher because of the outflow of vesicle content into the surrounding aqueous phase, and finally the enhancement of ANTS fluorescence. Quantitative analysis was performed by means of eqn. (3) where the reference intensity corresponds to maximum fluorescence at complete dilution of the vesicle content.

All fluorescence measurements were carried out on a Perkin-Elmer LS-50 B spectrofluorimeter (Beaconsfield, England).

IR linear dichroism measurements

Samples were prepared by pipetting 100–200 μl of the respective SUV dispersion onto the surface of a ZnSe attenuated total reflection (ATR) crystal (70 × 10 × 5 mm^3 trapezoid, face angle 45°, six active reflections) and evaporating the water under a stream of warm air. While drying, the material was spread uniformly onto the crystal surface by gently stroking with the pipette tip. The amount of material corresponds to an average thickness of the dry film larger than 3 μm.

The ATR crystal was mounted into a commercial horizontal ATR holder (Graseby Specac, Kent, UK) that had been

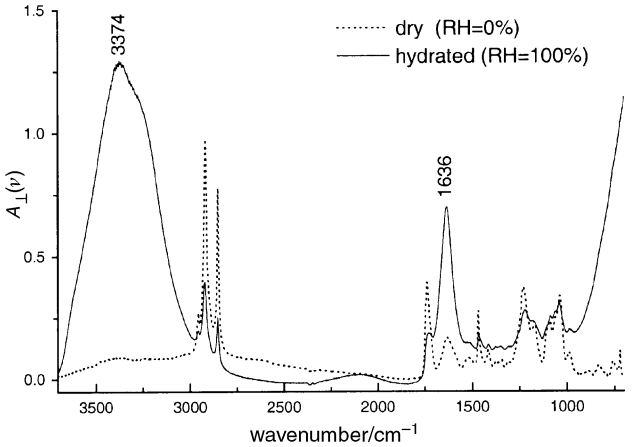

Fig. 1 Polarized IR spectrum of DMPS vesicles in 10 mM HEPES buffer (+100 mM NaCl, pH 7.5) after drying on the surface of the ZnSe-ATR crystal (···) and after rehydration in a saturated vapor atmosphere (——). The maximum position of the absorption bands due to the O–H stretching and H_2O bending modes of water are indicated in units of cm^{-1}.

modified so as to realize a well-defined relative humidity (RH) and temperature (T) within the sample chamber.[10] The dry lipid films were rehydrated in the thoroughly sealed sample chamber from vapor emanating from water-saturated filter paper of dimensions equivalent to those of the ATR crystal.[11] We expect that the lipid films fully hydrate in the saturated vapor atmosphere (RH ≈ 100%, see Fig. 1). The resulting molar ratio water-to-lipid, $R_{W/L} = 40–60$, was estimated from the absorbance ratio of the broad OH stretching band of water centered near 3390 cm^{-1} and the C=O stretching mode of DMPS at 1730 cm^{-1} (see ref. 12 for details). Note that a considerable amount of water solvates the buffer and NaCl present in the sample. The lipids were investigated by means of increasing temperature using a flowing water thermostat (Julabo, Germany) to adjust the temperature in the range 0–60 °C with an accuracy of ±0.1 K. The heating rate was 2 K h^{-1}.

Polarized absorbance spectra, $A_\parallel(\nu)$ and $A_\perp(\nu)$ (128 scans, nominal resolution 2 cm^{-1}), were recorded by means of a BioRad FTS-60a Fourier-transform IR spectrometer (Digilab, MA, USA) at two perpendicular polarizations of the IR beam, parallel (∥) and perpendicular (⊥) with respect to the plane of incidence.

The IR order parameter, S_{IR}, of an absorption band is defined as the ensemble averaged second-order Legendre polynomial of the angle enclosed between the IR active transition moment and the normal of the surface of the ATR crystal

$$S_{IR} = \frac{1}{2}\langle 3\cos^2\theta_\mu - 1\rangle = \frac{R - K_1^\infty}{R + K_2^\infty} \quad (4)$$

It was determined from the dichroic ratio of the polarized absorbances, $R \equiv A_\parallel/A_\perp$, which were evaluated from $A_\parallel(\nu)$ and $A_\perp(\nu)$ by integration after baseline correction. The constants $K_1^\infty = 2$ and $K_2^\infty = 2.54$ refer to Harrick's "thick" film approximation.[13]

The peak positions and the center of gravity (COG) of the absorption bands were determined from the weighted sum spectrum $A(\nu) = A_\parallel(\nu) + K_2^\infty A_\perp(\nu)$.[14]

3. Results and discussion

Binding of AxV to BBPS vesicles and membrane surface hydrophobicity

Fig. 2 shows the apparent relative permittivity, ε_s, in the vicinity of the dansyl fluorophore which is assumed to reside in the headgroup region of BBPS LUV. A considerable decrease of

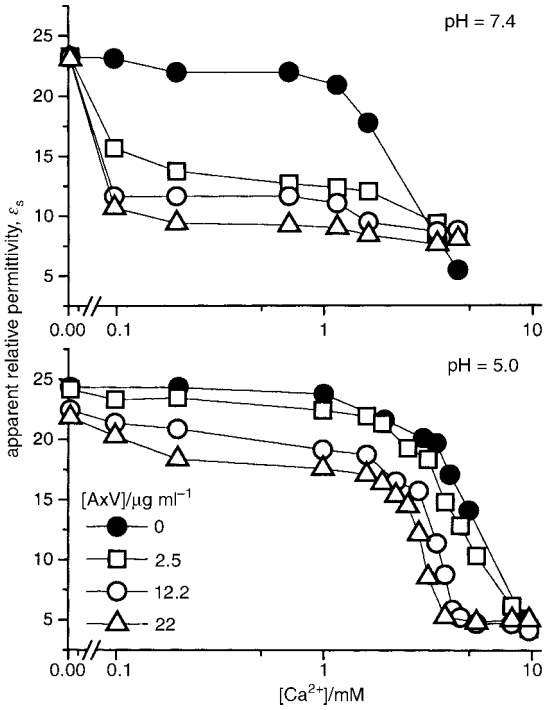

Fig. 2 Apparent surface relative permittivity, ε_s, of BBPS LUV ([L] = 100 μM) in the absence and presence of AxV as a function of the Ca^{2+} concentration (see figure for assignments). The pH was adjusted to pH 7.4 (above) and pH 5.0 (below) at T = 37 °C.

ε_s takes place beyond a threshold concentration of $[Ca^{2+}] > 1$ mM. The addition of AxV at pH 7.4 causes a drastic drop of ε_s already at small Ca^{2+} concentrations. At pH 5.0 AxV promotes the decrease of ε_s in a $[Ca^{2+}]$-dependent manner.

The decrease of the apparent surface relative permittivity is typically correlated with dehydration of lipid headgroups, and thus it indicates hydrophobization of the polar region of the bilayers. The results of our measurements reflect the fact that Ca^{2+} promotes the binding of AxV to negatively charged lipids in neutral conditions. After AxV binding the polar/apolar interface of the membranes becomes more hydrophobic. It was recently shown that the fusogenic potency of BBPS LUV correlates directly with their surface relative permittivity.[5] AxV promotes vesicle fusion at $0.1 \leqslant [Ca^{2+}]/\text{mM} \leqslant 1$ but inhibits fusion at 1.1 mM $\leqslant [Ca^{2+}]$ at pH 7.4 in correspondence with the ε_s measurements.

The mean hydrophobicity of AxV was estimated as a function of pH using a hydrophobicity scale proposed by Abraham and Leo[15] (Fig. 3). The pH-dependent charge of AxV corresponds to the degree of protonation of the amino acid side chains. Both, the charge and the mean hydrophobicity of the protein increase with decreasing pH. The latter tendency is expected to cause stronger binding of AxV at pH 5.0 due to the hydrophobic effect. Indeed, recent measurements of fluorescence resonance energy transfer between Trp-187 of AxV and a membrane-bound pyrene label show that the affinity of the protein for lipid vesicles increases with decreasing pH.[5] On the other hand, the smaller negative charge of AxV (and of PS) decreases the degree of calcium binding to AxV and PS. As a result the amount of calcium-mediated AxV–PS interactions is expected to weaken. In summary, the increased hydrophobicity of AxV at pH 5 explains that ε_s decreases slightly upon addition of AxV in the absence of Ca^{2+} whereas the relatively small effect of the divalent cations on ε_s at $[Ca^{2+}] < 1.2$ mM reflects the decreased role of coulombic lipid–protein interactions (Fig. 2, pH 5). These results show that binding of AxV to lipids becomes progressively driven by the hydrophobic effect with decreasing pH whereas the role of Ca^{2+}-mediated interactions decreases.

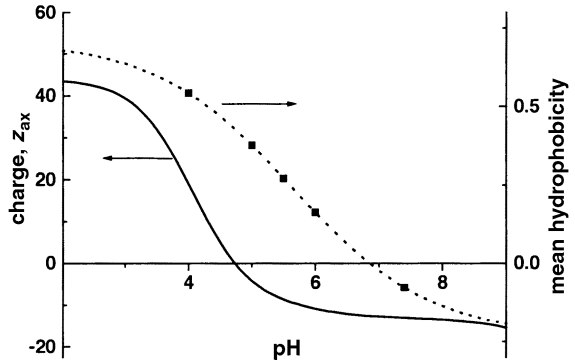

Fig. 3 Effective charge, z_{ax}, and mean hydrophobicity of AxV as a function of pH. z_{ax} represents the sum of the individual charges of the amino acid side chains which were calculated according to their pK_a. The "mean hydrophobicity" represents the average over the hydrophobicities of all side chains according to the hydrophobicity scale of Abraham and Leo.[13] It was calculated at selected pH values. The sigmoidal line (···) extrapolates the mean hydrophobicity to the whole pH range considered.

Surface charge of PS vesicles as a function of Ca^{2+} and AxV concentration

Table 1 summarizes the results of electrophoretic measurements on BBPS LUV. In the absence of AxV the surface charge of the negative BBPS vesicles increases with increasing Ca^{2+} concentration owing to the binding of cations. The change of the surface charge density yields the amount of calcium which binds to the lipid. The respective binding constant, $K \approx ([Ca^{2+}]_{bound}/[Ca^{2+}]0.5[L]) \approx 1.8\ M^{-1}$, corresponds to an intrinsic binding constant of $K_I \approx K \exp(2F\Psi_0/RT) \approx 10 \pm 2\ M^{-1}$ which agrees with previous results.[16] Here we assumed excess of free calcium, *i.e.* $[Ca^{2+}]_{bound} \ll [Ca^{2+}]$, [L].

AxV has no significant effect on the electrophoretic mobility and the mean size (not shown) of BBPS LUV in the absence of Ca^{2+}. We conclude that there is no significant binding of AxV to the vesicles because the protein is effectively negatively charged in neutral conditions, and thus its interaction with the lipid would decrease the apparent surface charge in contrast to the observations (see Fig. 3). This finding correlates with the invariant surface relative permittivity which was found upon addition of the protein at $[Ca^{2+}] = 0$ (*vide supra*). In contrast, continuous increase of σ_s with increasing AxV concentration was measured at acidic conditions (pH 4, not shown). This tendency reflects the binding of the positively charged protein to the vesicles owing to the hydrophobic effect.

The addition of Ca^{2+} causes a steeper increase of the ζ potential in the presence of the protein when compared with the sample without AxV (at neutral pH). If one interprets this effect exclusively in terms of surface electrostatics then it indicates that AxV promotes Ca^{2+} binding to the BBPS LUV. Note that AxV carries about 13 negative charges at pH 7.4 (Fig. 3) and potentially binds 5–12 Ca^{2+} ions.[17] After maximum Ca^{2+} binding AxV becomes positively charged ($z_{ax} \approx +10$) and thus complete binding of the protein to the vesicles would increase their apparent surface charge density by $\sigma_{ax} \approx 0.01$ As m^{-2}. This value agrees with the measured difference of σ_{ap} between BBPS LUV in the presence and absence of AxV. Hence, the respective change in electrophoretic mobility can be explained by complete binding of the protein to the lipid.

Fluorescence quenching studies on penetration of AxV into PS membranes

Fig. 4 shows the efficiency of quenching of tryptophan fluorescence of AxV by doxyl spin probes which were attached at different positions of the C18-acyl chains of a PC lipid which was mixed with BBPS. At pH 7.4 there is no significant effect in the absence of Ca^{2+} owing to the weak binding of AxV. After the addition of calcium ions about 50% of the Trp-187 fluorescence intensity becomes quenched by the doxyl groups in position 5 which are located near the glycerol moiety of the lipid. The quenching efficiency decreases with increasing distance of the doxyl groups from the polar interface. These results show that the Trp-187 residue of membrane bound AxV is located within the hydrophobic core of the bilayer with highest probability in the vicinity of the glycerol groups of the lipid. The considerable quenching efficiency of doxyl groups in position 16 can be explained by a broad distribution of AxV positions ranging from the lipid/water interface to the bilayer center or, alternatively, by a certain amount of chain "upturns" of the fluid acyl chains of the lipid which are partially caused by the doxyl labels tending to approach the polar interface. At pH 5 the efficiency of quenching is much smaller because of the weaker binding of the protein to the vesicles. Note that increased hydrophobicity causes interaction of AxV with the lipids even in the absence of Ca^{2+}.

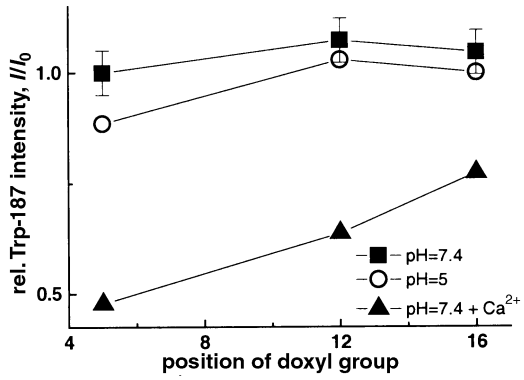

Fig. 4 Relative fluorescence intensity of Trp-187 fluorescence of AxV in mixed BBPS–doxyl-PC LUV (1 : 1 mole/mole; 100 μM) as a function of the position of the doxyl groups in the C18-chain of the spin-labeled PC lipid. The fluorescence intensity in the presence of the quencher is denoted by I and the respective intensity in pure BBPS LUV without quencher by I_0. The pHs were 7.4 and 5 (see figure), the AxV concentration 20 μg ml^{-1}, the Ca^{2+} concentration 100 μM and the temperature 37 °C.

Table 1 ζ potential and apparent surface charge density of BBPS large unilamellar vesicles and concentration of membrane-bound Ca^{2+} in the absence and presence of AxV[a]

$[Ca^{2+}]$ /μM	ζ/mV		$\sigma_{ap}{}^{b}/10^{-3}$ A s m^{-2}		$[Ca^{2+}]_{bound}$/μM	
	PS	PS + AxV	PS	PS + AxV	PS	PS + AxV
0	−42 ± 5	−42 ± 5	−44 ± 5	−44 ± 5	—	—
100	−36 ± 5	−27 ± 5	−36 ± 5	−26 ± 5	0.013	0.030
200	−30 ± 5	−22.5 ± 5	−29 ± 5	−21 ± 5	0.025	0.038

[a] Lipid concentration: [L] = 150 μM; AxV concentration: 10 μg ml^{-1} (0.33 μM); pH 7.4; 100 mM NaCl. [b] See eqn. (1) and (2).

Accessibility of Trp-187 for the aqueous medium was studied by means of the water-soluble quencher acrylamide the concentration of which was varied between 0 and 150 mM (pH 7.4). The quenching of Trp-187 fluorescence of (i) AxV, (ii) AxV + 38 mM Ca^{2+} and (iii) AxV + 200 μM BBPS LUV + 200 μM Ca^{2+} was well described by linear Stern–Volmer plots of different slopes yielding Stern–Volmer constants of (i) 10 M^{-1}, (ii) 18 M^{-1} and (iii) 7 M^{-1} (not shown). These results indicate that the interaction of Ca^{2+} with AxV in the absence of lipid membranes exposes the tryptophan residues to the aqueous phase. The tryptophan residues however bury in the bilayers upon Ca^{2+} mediated binding of AxV to BBPS LUV, and consequently they become much less accessible to water soluble quencher. This result is compatible with the quenching of Trp-187 by doxyl labels near the glycerol group reported above.

Leakage and content-mixing of lipid vesicles after interaction with AxV and/or Ca^{2+}

Calcium ions and/or AxV induce moderate leakage of the BBPS vesicles (10–25%) at neutral pH (Table 2). Considerable outflow of the vesicle content only takes place at relatively high Ca^{2+} concentration (4 mM). AxV inhibits leakage in these conditions. In contrast, the protein promotes leakage in the presence and absence of Ca^{2+} at acidic pH. The addition of AxV affects contents-mixing of vesicles in a similar manner to their leakage. That means, the protein inhibits mixing at pH 7.4 and promotes mixing at pH 4.0 (Table 2, see data given in parentheses). Mixing is however less effective in the presence of AxV, moderate Ca^{2+} concentration (0.4 mM) and pH 7.4 when compared with leakage.

The leakage assay gives a measure of the potency of additives to destroy the integrity of vesicles which can be thought to lose their content upon transformation into multibilayer stacks. In contrast, the content-mixing assay estimates fusogeniety, *i.e.*, the merging of vesicles to larger ones without leakage of their bilayer envelopes. The similar results of both assays indicate that leakage and fusion are correlated in the investigated systems. In other words, fusion and destabilization of bilayers are closely related effects. The degree of fusion was less than 25% in all systems studied whereas leakage reaches 70–80%. Hence, the additives AxV and/or Ca^{2+} cause the destruction of vesicles in the first place and their fusion only to a weaker degree. Note that the presence of AxV additionally destabilizes the membranes at moderate Ca^{2+} concentrations (~0.4 mM).

The effect of AxV and/or of Ca^{2+} on the chain-melting transition of DMPS

Fig. 5 and 6 show the COG, and the IR order parameter, S_{IR}, of the symmetric methylene stretching band, $\nu_s(CH_2)$, of a series of sample films on the ATR crystal surface that were heated in a saturated vapor atmosphere (RH = 100%). We studied the lipid (DMPS) in the presence and absence of Ca^{2+}

Table 2 Leakage (and contents-mixing), *D*, of BBPS large unilamellar vesicles at variable AxV and Ca^{2+} concentrations[a]

	pH 7.4		pH 4.0	
[AxV] =	0 μg ml^{-1}	10 μg ml^{-1}	0 μg ml^{-1}	10 μg ml^{-1}
[Ca^{2+}] =				
0 mM	0(0)	10(0)	0(0)	75(5)
0.4 mM	4(2)	21(0)	3(3)	70(10)
4.0 mM	70(20)	25(0)	68(25)	80(10)

[a] *Cf.* eqn. (3), in units of %; lipid concentration [L] = 100 μM; *T* = 37 °C; error ±5%.

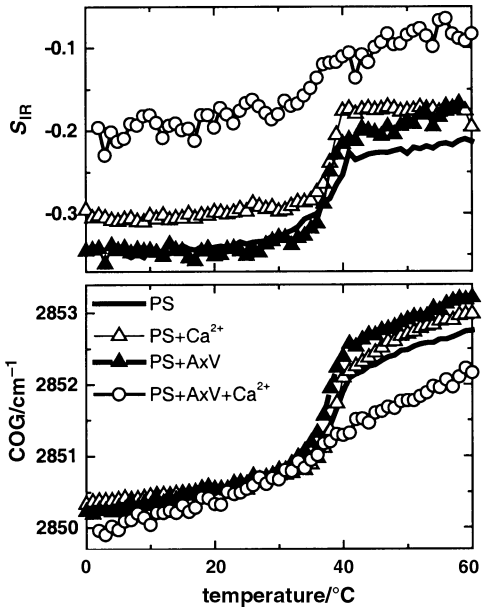

Fig. 5 S_{IR} (above), COG (below), of the symmetric methylene stretching vibration of DMPS films and mixtures of DMPS (PS) with Ca^{2+} and/or AxV (AxV, assignments of the symbols are given in the figure) as a function of temperature. The films were prepared from vesicle suspensions (pH 7.4) and rehydrated at RH = 100%. Molar ratios Ca^{2+}-to-lipid and AxV-to-lipid were 0.2 and 0.4, respectively.

(molar ratio Ca^{2+}-to-DMPS $R_{Ca/L} = 0.2$) and/or AxV (molar ratio protein-to-DMPS $R_{Ax/L} = 0.4$). The sigmoidal increase of both spectral parameters, $S_{IR}(\nu_s(CH_2))$ and $COG(\nu_s(CH_2))$, is typical for the main phase transition at which the lipid transforms from the gel to the liquid-crystalline phase.[11,18,19] This order–disorder transition involves primarily the conformational melting of the fatty acyl chains. Their stretched all-*trans* conformation in the gel state becomes evident from the existence of the CH_2 wagging band progression below the phase transition temperature, T_m (see below). The temperature of the phase transition, T_m, is conveniently determined from the

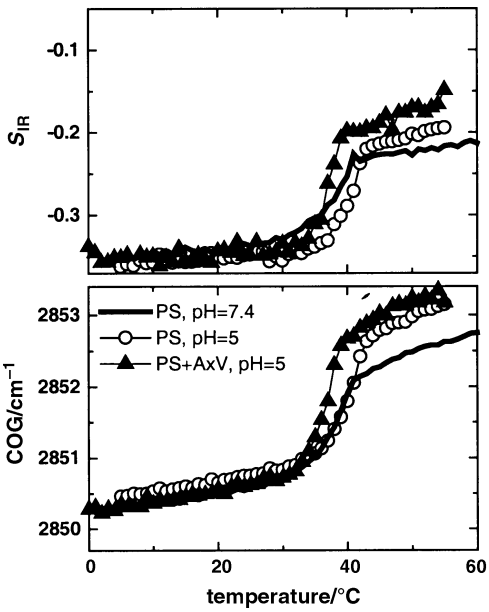

Fig. 6 S_{IR} (above), COG (below), of the symmetric methylene stretching vibration of DMPS films and of a mixture of DMPS with AxV (assignments of the symbols are given in the figure) as a function of temperature. The films were prepared from vesicle suspensions at pH 7.4 and 5.0 and rehydrated at RH = 100%. Molar ratios Ca^{2+}-to-lipid and AxV-to-lipid were 0.2 and 0.4, respectively.

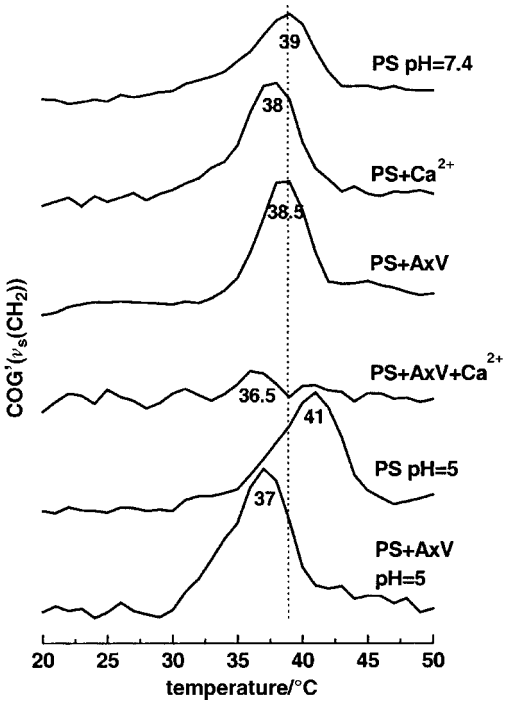

Fig. 7 First derivative of the COG graphs shown in Fig. 5 and 6. The numbers give the maximum position of the peaks in units of °C with a resolution of ±0.5 K. The position of the gel-to-liquid-crystalline phase transition of pure DMPS is indicated by the vertical dotted line.

maximum of the first derivative $COG' = \partial COG(\nu_s(CH_2))/\partial RH$ that is shown in Fig. 7.

At pH 7.4 we found the transition of pure DMPS at exactly the same temperature $T_m = 39\,°C$ as has been detected previously by means of differential scanning calorimetry and X-ray analysis.[20] Because these samples were studied in aqueous buffer solution (+100 mM NaCl) we concluded that our conditions guarantee full hydration of the lipid in agreement with previous results.[11]

The addition of Ca^{2+} to DMPS has nearly no effect on the phase transition temperature of the lipid (Fig. 7). This result is somewhat surprising because Ca^{2+} and DMPS form a crystalline Ca^{2+}–DMPS complex under certain conditions. The bilayer structure is preserved in this so-called cochleate phase, but the gel to liquid-crystalline phase transition occurs at much higher temperatures than in pure DMPS.[20–23] Spectral analysis indicates a considerable interaction of Ca^{2+} with the phosphate groups of DMPS in our samples also (see below). We suggest that formation of bidental Ca^{2+} bridges between the headgroups of opposite monolayers is prevented by unknown reasons. Crystalline precipitates of charged lipid and calcium cations are thought to consist in a two-dimensional network where the lipid molecules of adjacent bilayers are separated by a plane of calcium ions.[24] Such *cis*-bridges are probably essential for the stability of the complexes, and thus for the upwards shift of T_m.

Addition of AxV to the membranes in the absence of divalent cations under neutral conditions leaves the phase transition of DMPS virtually unchanged. This result reflects weak binding of the protein to the bilayer in agreement with the results of fluorescence and electrophoretic measurements (*vide supra*). The phase transition of DMPS disappears nearly completely in the presence of both additives AxV *and* Ca^{2+}. Obviously specific ternary interactions between DMPS, AxV and Ca^{2+} stabilize the lipid in the gel state. This result corresponds with recent findings that complex formation between DMPA, Ca^{2+} and AxV cause marked rigidization of DMPA monolayers.[25]

The COG of the methylene stretching band and the respective IR order parameter are suitable estimates of the conformational and macroscopic order of the acyl chains of the lipids. The increase of both parameters after the addition of AxV *or* Ca^{2+} at $T > T_m$ indicates a slight disordering of the lipid chains in comparison with pure DMPS (Fig. 5). The larger values of $S_{IR}(\nu_s(CH_2))$ in the gel phase of DMPS + Ca^{2+} should be attributed to a more disturbed macroscopic alignment of the multibilayer stacks with the ATR surface because the $\nu_s(CH_2)$ frequencies of pure DMPS and of DMPS + Ca^{2+} are nearly equal. The same argument applies to the DMPS + AxV + Ca^{2+} sample which however remains in the gel state up to 60 °C. This result is evidenced by IR spectra which show the methylene wagging band progression over the whole temperature range studied (*vide infra*).

The effect of pH on the chain melting transition of DMPS

The lowering of the pH to pH 5.0 causes the upwards shift of the phase transition to $T_m = 41\,°C$ (Fig. 7) and a slight disordering of the fatty acid chains in the liquid-crystalline phase (Fig. 6). On the basis of the pH-titration curve of PS given in ref. 26 and 27 we estimate that about 30% of the COO^- groups present at pH 7.4 become protonated at pH 5.0. This hypothesis is confirmed by the observation that the ratio of the integral absorbances of the $\nu_{as}(COO^-)$ and the ν(C=O) bands (assignments of the bands are given below) is about 20% smaller at pH 5.0 than at pH 7.4. The repulsive coulombic forces between the phosphatidylserine headgroups are expected to decrease on average in more acidic conditions because of the smaller fraction of negatively charged lipid molecules. This tendency stabilizes the gel phase, and thus increases T_m in accordance with our and previous[28] experimental results.

In contrast to the phase behavior at neutral pH the addition of AxV significantly decreases T_m at pH 5.0 (Fig. 7). This result is in accordance with the fluorescence measurements reported above. The binding ability of phosphatidylserine vesicles for AxV is higher at low pH because partial protonation of the acidic residues of the protein increases its hydrophobicity (Fig. 3 and ref. 5). It was suggested that AxV is able to penetrate the membrane at low pH owing to the hydrophobic effect. The slightly increased values of $S_{IR}(\nu_s(CH_2))$ and $COG(\nu_s(CH_2))$ in the DMPS + AxV samples at pH 5.0 and $T > T_m$ (compare Fig. 5 and 6) possibly reflect the disordering of the hydrophobic core of the bilayer after incorporation of AxV.

IR spectrum of dried DMPS in the presence and absence of Ca^{2+} and/or AxV

The IR spectra of phosphatidylserines in the presence and absence of Ca^{2+} or other cations are well characterized. For a general review we refer to ref. 29 and the references cited therein. It was found that Ca^{2+} ions mainly interact with the phosphate groups leading to their dehydration, immobilization and to a conformational change of the phosphodiester moiety from *gauche/gauche* to *trans/trans*.[19,30,31] After the addition of Ca^{2+}, these effects are clearly indicated in our DMPS samples by the narrowing and shift of the antisymmetric PO_2^- and $P–(OC)_2$ stretches near 1230 cm^{-1} ($\nu_{as}(PO_2^-)$) and 832 cm^{-1} ($\nu_{as}(P–(OC)_2)$), respectively, and by the appearance of satellite bands, for example at 1109 cm^{-1}, which probably originates from a C–(OP) stretching mode (see Fig. 8).

The C=O stretching band centered at 1738 cm^{-1} in pure DMPS splits into a complex pattern of at least four distinguishable peaks at 1741, 1730, 1721 and 1713 cm^{-1} in the presence of Ca^{2+}. The splitting was explained by different rotational chain isomers, by strong hydrogen bonding to trapped interstitial water and to the hydration shell of Ca^{2+}

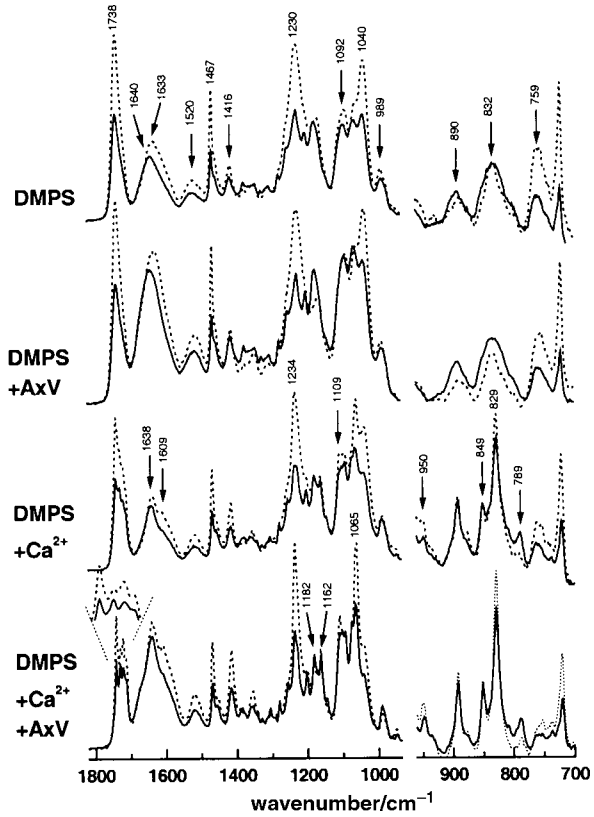

Fig. 8 Polarized IR spectra, $A_{\parallel}(\nu)$ (solid line) and $2A_{\perp}(\nu)$ (dotted line), of DMPS in the presence of AxV or/and Ca^{2+} in dry lipid films. Note that the condition $A_{\parallel}(\nu) = 2A_{\perp}(\nu)$ refers to the absence of molecular order of the respective transition moment, or alternatively, to its orientation with the magic angle ($\sim 54.7°$) relative to the normal of the ATR surface. The position of selected absorption bands is given in units of cm^{-1}.

and by nonequivalent anchoring of the sn-1 and sn-2 chains to the glycerol group.[32,33] Hence, there is clear indication of characteristic complex formation between the metal ions and the lipid despite the virtually unchanged phase behavior of DMPS after addition of Ca^{2+} (*vide supra*).

The negatively charged carboxylate group in the serine moiety gives rise to a doublet near 1640 and 1416 cm^{-1} due to the antisymmetric and symmetric COO^- stretching modes, $\nu_{as}(COO^-)$ and $\nu_s(COO^-)$, respectively. The different peak positions of the band centered at 1640 cm^{-1} in the $\parallel$ and $\perp$ polarized spectra clearly indicate that this feature represents the composite of at least two differently oriented transition moments. The second one at the low-frequency side can be assigned to the antisymmetric bending mode of the NH_3^+ group, $\delta_{as}(NH_3^+)$.[31] Both composite bands narrow in the presence of Ca^{2+}, indicating the immobilization of the NH_3^+ and COO^- moieties.

The presence of AxV causes the enhancement of the features at 1640 and 1520 cm^{-1} due to the amide I and amide II bands of the protein which are expected to overlap with the $\nu_{as}(COO^-)$ and $\delta_s(NH_3^+)$ bands, respectively.[34]

AxV obviously "amplifies" the effect of Ca^{2+} on the spectrum of DMPS: The phosphate bands further narrow, the shoulder at 1109 cm^{-1} protrudes more clearly and the complex peak pattern of the ν(C=O) mode increases in intensity.

IR linear dichroism of the phosphatidylserine headgroups

The polarized spectra of DMPS reveal the mean orientation of the phosphatidylserine groups with respect to the membrane surface (Fig. 8). Most of the absorption bands possess perpendicular linear dichroism, *i.e.* $A_{\parallel} < 2A_{\perp}$. The IR order parameters of the $\delta_s(NH_3^+)$ and $\nu_s(COO^-)$ bands, $S_{IR}(\delta_s(NH_3^+)) = -0.1$ and $S_{IR}(\nu_s(COO^-)) = -0.15$, indicate the in-plane alignment of the respective transition moments which point along the C_{3v} and C_{2v} symmetry axes of the NH_3^+ and COO^- moieties, respectively. The values of $S_{IR}(\nu(C{=}O)) = -0.25$ and $S_{IR}(\nu_{as}(PO_2^-)) = -0.25$ are typical for the in-plane orientation of the C=O bond and of the interconnecting line between the two non-esterified oxygens, respectively. The IR order parameter of the $\nu_{as}(P(OC)_2)$ band represents a marker of the mean orientation of the C–O–P–O–C backbone because its transition moment roughly points along the interconnecting line between the two esterified oxygens.[35,36] In membranes of lipids with phosphatidylcholine headgroups $S_{IR}(\nu_{as}(P(OC)_2))$ is typically positive because of the oblique orientation of the PC headgroup with respect to the membrane plane.[37] In contrast, the PS headgroup points more parallel with respect to the membrane surface, as indicated by $S_{IR}(\nu_{as}(P(OC)_2)) = 0$.

After addition of Ca^{2+} and/or AxV the linear dichroism, and thus also the mean orientation of the PS groups, remains virtually unchanged. A slight decrease of the (negative) values of $S_{IR}(\delta_s(NH_3^+))$ and $S_{IR}(\nu_s(COO^-))$ in the presence of Ca^{2+} can be explained by the immobilization of the respective moieties.

The spectrum of diacyl phospholipids is characterized by an intense, strongly dichroic feature in the range 1150–1000 cm^{-1}. It can be assigned to the superposition of the symmetric PO_2^- stretching vibration ($\nu_s(PO_2^-)$) near 1092 cm^{-1} with symmetric ester bond stretches of the acyl chains ($\nu_s(COC)$) near 1065 cm^{-1} and with a stretching mode of the phosphodiester group ($\nu(COP)$) at 1040 cm^{-1}. The binding of Ca^{2+} to the lipid gives rise to the marked enhancement of the $\nu_s(COC)$ band the dichroism of which becomes clearly perpendicular. This tendency is accompanied by a narrowing of the respective antisymmetric COC stretches ($\nu_{as}(COC)$) at 1182 cm^{-1} and 1162 cm^{-1} which can be assigned to the ester bonds in the sn-1 and sn-2 chains, respectively, because of their different conformation and orientation in membranes of diacyl lipids.[38,39] Hence, immobilization of the PS headgroups after Ca^{2+} binding also involves the carbonyl-ester groups, and thus the whole polar region of the DMPS bilayers becomes rigid owing to interaction with the metal cations.

IR spectrum of fully hydrated DMPS before and after interaction with Ca^{2+} and/or AxV

Fig. 9 shows the polarized spectra of fully hydrated samples in the spectral window which is free of strong absorption bands of water. The essential spectral and dichroic features of the investigated systems remain virtually unchanged after hydrating the films. The all-*trans* conformation of the acyl chains below the phase transition temperature is evidenced by the CH_2 wagging progression in the range 1180–1340 cm^{-1} (Fig. 9, arrows). This series of equally spaced bands is still present in the DMPS + AxV + Ca^{2+} sample up to 60 °C. The considerable weakening of the bands indicates that the all-*trans* conformation of an increasing fraction of the chains is disturbed by defects upon heating.

Progressive hydration of the phosphate groups of phospholipids causes a characteristic shift of the $\nu_{as}(PO_2^-)$ band towards smaller frequencies. Therefore this mode is well suited as a marker of the hydration state of the PO_2^- group of PS.[27,40] The phosphate band of DMPS at 1222 cm^{-1} corresponds to fully hydrated headgroups in the presence and absence of AxV. Calcium ions dehydrate the phosphate group of PS lipids in a concentration dependent manner.[23,40] ^{2}H-NMR spectra[23] and the shape of the $\nu_{as}(PO_2^-)$ band[40] reveal that the PS membrane can be viewed as a partially phase-separated two-component mixture of partially dehydrated PS/Ca^{2+} complexes and hydrated lipid molecules

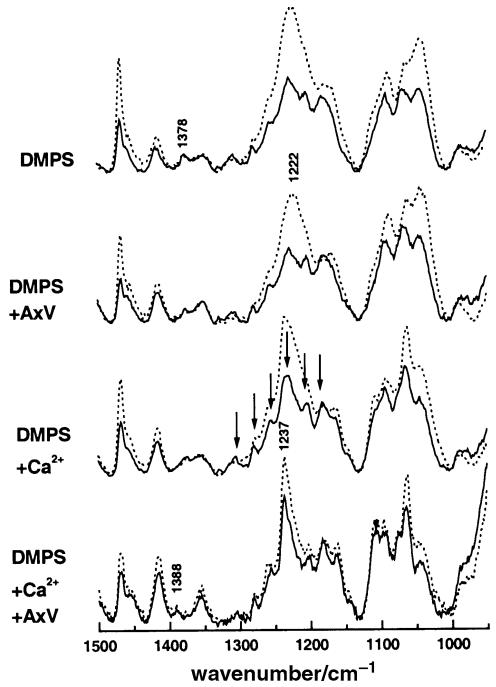

Fig. 9 Polarized IR spectra, $A_{\parallel}(\nu)$ (solid line) and $2A_{\perp}(\nu)$ (dotted line), of DMPS in the presence of AxV or/and Ca^{2+} in fully hydrated lipid films at $T = 20\,^{\circ}C$.

below a saturation limit of PS : $Ca^{2+} \approx 2:1$ mol/mol, the value which corresponds to the stoichiometry of the complex. The dehydrated complex is characterized by a narrow $\nu_{as}(PO_2^-)$ band near 1237 cm^{-1}. The position and width of the phosphate band of DMPS in the presence of AxV and Ca^{2+} indicates that the predominant fraction of PO_2^- groups is dehydrated. In the DMPS + Ca^{2+} sample the maximum of $\nu_{as}(PO_2^-)$ remained at 1237 cm^{-1}, but the band was considerably widened, indicating that besides dehydrated PO_2^- groups a considerable fraction of hydrated ones still exists. We conclude that the observed phase transition of the DMPS + Ca^{2+} films is caused mainly by the fraction of the lipid which does not strongly interact with the divalent metal cations. Preliminary studies show that the area of the peak of $COG'(\nu_s(CH_2))$ (Fig. 7) gradually decreases at higher Ca^{2+} concentrations (unpublished).

Other IR-spectroscopic marker bands can also be used to estimate the amount of DMPS which is involved in complex formation with Ca^{2+}.[22] It was shown that dehydration of the phosphate groups precedes the formation of a cochleate phase which involves the normally insensitive methyl symmetric deformation mode.[22] In the absence of Ca^{2+} this mode is centered at 1378 cm^{-1} (Fig. 9). The band shifts upwards by 8–10 cm^{-1} in the DMPS + AxV + Ca^{2+} sample and represents a superposition of both features in the DMPS + Ca^{2+} film. Hence, the IR spectrum gives evidence that the cochleate phase of DMPS is induced by both additives, Ca^{2+} and AxV.

The results show that AxV promotes interaction of Ca^{2+} with the membranes at full hydration in a similar fashion as was found in the dried films.

4. Summary and conclusions

In neutral conditions ternary complex formation between the anionic binding sites of AxV, negatively charged phosphatidylserine headgroups and calcium ions stabilizes the gel state of the lipid. The protein penetrates into the bilayers causing a considerable decrease in the apparent surface relative permittivity. The stability of PS vesicles is affected in a moderate fashion only. In contrast, AxV binding to PS at acidic conditions destroys their integrity to a high degree. In addition, disordering of the lipid acyl chains accompanies the destabilization of the gel phase. These effects can explained the increased hydrophobicity of the protein at low pH.

Hence, binding of AxV to lipids becomes progressively driven by the hydrophobic effect with decreasing pH whereas the role of Ca^{2+}-mediated interactions decreases. This tendency is paralleled by the progressive destabilization of the bilayers and, to a lesser extent, by an increased tendency of the vesicles to merge into larger ones. We suggest that a peripheral calcium-mediated insertion mode of AxV at neutral pH shifts towards a more integral one at acidic pH.

AxV promotes interaction of Ca^{2+} with the membranes, and thus the effect of the divalent cations on the membranes is obviously amplified in the presence of macromolecules. Ternary complex formation between an anionic polymer, calcium ions and lipid membranes was reported also to increase the packing density and molecular order of the lipids in other systems.[41] Calcium-mediated association of macromolecules to membranes can be alternatively viewed as a polymer-mediated binding of divalent cations to the lipid which promotes complex formation between the ions and lipid headgroups.

Acknowledgements

This work was supported by the Deutsche Forschungsgemeinschaft within SFB 197/TP A10.

References

1 P. Raynal and H. B. Pollard, *Biochim. Biophys. Acta*, 1994, **1197**, 63.
2 N. O. Concha, J. F. Head, M. A. Kaetzel, J. R. Dedman and B. A. Seaton, *Science*, 1993, **261**, 1321.
3 A. Brisson, G. Mosser and R. Huber, *J. Mol. Biol.*, 1991, **220**, 199.
4 M. A. Swairjo, M. F. Roberts, M. B. Campos, J. R. Dedman and B. A. Seaton, *Nat. Struct. Biol.*, 1994, **2**, 968.
5 G. Köhler, U, Hering, O. Zschörnig and K. Arnold, *Biochemistry*, 1997, **36**, 8189.
6 B. R. Genge, L. N. Y. Wu, H. D. Adkisson and R. E. Wuthier, *J. Biol. Chem.*, 1991, **266**, 10678.
7 M. Eisenberg, T. Gresalfi, T. Riccio and S. McLaughlin, *Biochemistry*, 1979, **18**, 5213.
8 S. Ohki and K. Arnold, *J. Membr. Biol.*, 1990, **114**, 195.
9 H. Ellens, D. P. Siegel, D. Alford, P. L. Yeagle, L. Boni, L. J. Lis, P. J. Quinn and J. Bentz, *Biochemistry*, 1989, **28**, 3692.
10 H. Binder, A. Anikin, B. Kohlstrunk and G. Klose, *J. Phys. Chem. B*, 1997, **101**, 6618.
11 H. Binder, *Vib. Spectrosc.*, 1999, **21**, 151.
12 H. Binder, K. Arnold, A. S. Ulrich and O. Zschörnig, submitted.
13 N. J. Harrick, *Internal Reflection Spectroscopy*, Wiley, New York, 1967.
14 H. Binder and H. Schmiedel, *Vib. Spectrosc.*, 1999, **21**, 51.
15 D. J. Abraham and A. J. Leo, *Proteins*, 1987, **2**, .
16 S. McLaughlin, N. Mulrine, T. Gresalfi, G. Vaio and A. McLaughlin, *J. Gen. Physiol.*, 1981, **77**, 445.
17 R. Huber, M. Schneider, I. Mayr, J. Römisch and E. P. Paques, *FEBS Lett.*, 1990, **275**, 15.
18 H. L. Casal and H. H. Mantsch, *Biochim. Biophys. Acta*, 1984, **779**, 381.
19 H. L. Casal, H. H. Mantsch and H. Hauser, *Biochemistry*, 1987, **26**, 4408.
20 H. Hauser, F. Paltauf and G. G. Shipley, *Biochemistry*, 1982, **21**, 1061.
21 H. Hauser, I. Pascher, R. H. Pearson and S. Sundell, *Biochem. Biophys. Acta*, 1981, **650**, 21.
22 C. R. Flach and R. Mendelsohn, *Biophys. J.*, 1993, **64**, 1113.
23 M. Roux and M. Bloom, *Biophys. J.*, 1991, **60**, 38.
24 G. Laroche, E. J. Dufourc, J. Dufourcq and M. Pezolet, *Biochemistry*, 1991, **30**, 3105.
25 F. Wu, A. Gericke, C. R. Flach, T. R. Mealy, B. A. Seaton and R. Mendelsohn, *Biophys. J.*, 1998, **74**, 3278.
26 F. Lopez-Garcia, J. Villalain, J. Gomez-Fernandez and C. Juan, *Biochim. Biophys. Acta*, 1995, **1236**, 279.

27 J. C. Gomez-Fernandez and J. Villalain, *J. Chem. Phys. Lipids*, 1998, **96**, 41.
28 G. Cevc, *Biochemistry*, 1987, **26**, 6305.
29 W. Hübner and A. Blume, *Chem. Phys. Lipids*, 1998, **96**, 99.
30 H. L. Casal, H. H. Mantsch, F. Paltauf and H. Hauser, *Biochim. Biophys. Acta*, 1987, **919**, 275.
31 K. Leberle, I. Kempf and G. Zundel, *Biophys. J.*, 1989, **55**, 637.
32 R. A. Dluhy, D. G. Cameron, H. H. Mantsch and R. Mendelsohn, *Biochemistry*, 1983, **22**, 6318.
33 W. Hübner, H. H. Mantsch, F. Paltauf and H. Hauser, *Biochemistry*, 1994, **33**, 320.
34 F. Wu, C. R. Flach, B. A. Seaton, T. R. Mealy and R. Mendelsohn, *Biochemistry*, 1999, **38**, 792.
35 U. P. Fringeli and H. H. Günthard, *Mol. Biol. Biochem. Biophys.*, 1981, **31**, 270.
36 H. Binder, T. Gutberlet, A. Anikin and G. Klose, *Biophys. J.*, 1998, **74**, 1908.
37 H. Binder, K. Arnold, A. S. Ulrich and O. Zschörnig, *Biochim. Biophys. Acta*, 2000, in the press.
38 U. P. Fringeli, *Z. Naturforsch. C*, 1977, **32**, 20.
39 H. Binder, A. Anikin, G. Lantzsch and G. Klose, *J. Phys. Chem. B*, 1999, **103**, 461.
40 F. Lopez-Garcia, V. Micol, J. Villalain and J. Gomez-Fernandez, *Biochim. Biophys. Acta*, 1993, **1169**, 264.
41 D. Huster, G. Paasche, U. Dietrich, O. Zschörnig, T. Gutberlet, K. Gawrisch and K. Arnold, *Biophys. J.*, 1999, **77**, 879.